The Monte Carlo Method: Versatility Unbounded In A Dynamic Computing World
Chattanooga, Tennessee, April 17–21, 2005, on CD-ROM, American Nuclear Society, LaGrange Park, IL (2005)

A CASE STUDY ON PATIENT EFFECTIVE DOSES DURING PROTON RADIATION TREATMENT

Hongyu Jiang, Harald Paganetti, Herman Suit
Department of Radiation Oncology
Massachusetts General Hospital and Harvard Medical School
Boston, MA 02114 USA
hjiang3@partners.org; hpaganetti@partners.org; suit.herman@mgh.harvard.edu

Brian Wang, X. George Xu
Nuclear Engineering and Engineering Physics
Rensselaer Polytechnic Institute
Troy, NY 12180, USA
wangb@rpi.edu; xug2@rip.edu

ABSTRACT

Cancer patients undergoing radiation treatment are exposed to primary and secondary radiation delivering relatively low doses to organs away from the targeted tumor. In the case of proton therapy, secondary neutrons generated from the accelerator head and inside the patient can reach many areas in the patient body. Due to the improved management of cancer patients, the number of long term survivors post radiation treatment is increasing substantially. This results in a mounting concern about the risk of radiation induced cancer appearing at late post treatment times. This paper presents a case study to determine the effective dose of patients undergoing proton treatment procedures. A whole-body patient model, VIP-Man was employed as the patient model. The VIP-Man dataset was implemented into the GEANT4 Monte Carlo code. Two proton treatment plans for the lung tumor and the paranasal sinus were simulated. The organ doses and ICRP-60 radiation and tissue weighting factors were used to calculate the effective dose. Results show that the whole body effective dose for the two proton plans is 5.8 rem and 0.4 rem, respectively.

Key Words: secondary dose, neutron, proton therapy, GEANT4, VIP-Man

1. INTRODUCTION

Radiation therapy is a major treatment option for a variety of cancers. Currently, about 50% to 60% of cancer patients are treated with radiation at some point in the course of their disease [1]. Probability of cure of cancer patients has been regularly improving with the consequence of increasing numbers of long term survivors. This has increased the concern of the risk of late radiation injury, especially that of radiation induced cancer. Cancer incidence as a result of radiation treatment is an emerging topic of interest because radiation has been identified as one of the three major factors (radiation, chemicals, and viruses or bacteria) that contribute cancer development [2]. The goal of radiation treatment planning is to design field number and array (static or dynamic) and beam characteristics so as to minimize radiation dose to tissues outside the planned high dose treatment volume. The planning tumor volume (PTV) is defined as the tissue volume to receive the planned target dose. The organs at risk (OARs) are defined as the

organs to outside of the PTV and the dose to which should receive a dose as near to zero as technically feasible. The dose to the OARs is high close to the PTV and decreases with distance to the further most part of the body. In present treatment planning technique, only organs that are situated next to the tumor are included in the OARs assuming that the secondary radiation delivers no or a relatively small amount of dose to organs not close to the target. However, the link of stochastic effects of relatively low doses of radiation to long-term increase of cancer incurrence is known [3]. Interestingly, new clinical treatment procedures, such as IMRT (Intensity Modulated Radiation Therapy), irradiate larger volumes of tissue to intermediate dose levels than conventional photon treatment, thus increasing the amount of secondary dose exposures to patients.

In radiation treatment, the primary radiation is collimated to achieve the required beam cross-section and the steepest dose gradient at the field edge. The major source of the irradiation beyond the PTV is the secondary particles generated in the pathways of the primary beam via atomic and nuclear interactions. These secondary particles include neutrons and photons that can travel larger distances from the site of their production to deposit radiation energies to the healthy tissues.

Radiation treatment with high-energy heavy charged particles has the clear advantage relative to photon beams. Because of sharp fall-off at the end of the spread-out Bragg peak, there can be important reduction in doses to OARs and the integral dose. At Northeast Proton Therapy Center (NPTC), Massachusetts General Hospital (MGH), more than 1000 patients have been treated by proton beam methods. With the high energy of the incident protons (up to 235 MeV), the major concern in secondary dose calculation is secondary neutrons following proton nuclear reactions [4,5].

Monte Carlo method can provide the most accurate radiation dose calculations. The flexibility and accuracy of it make the Monte Carlo method an excellent tool to study the secondary dose deposition because a detailed measurement is often time consuming, costly, or impossible under some circumstances. At NPTC, we have successfully developed GEANT4 based Monte Carlo methods to recalculate proton treatment plans (using a pencil beam algorithm) and to compare the Monte Carlo simulated dose distributions to the planned dose distributions [6,7]. This Monte Carlo method makes calculation of the neutron-induced dose in organs beyond the PTV straightforward.

A patient model is necessary in this study. Most CT scans of a patient cover only a small portion of the body and it is impossible to calculated dose to organs outside of the CT scan. The Rensselaer Radiation Measurement and Dosimetry Group (RRMDG.rpi.edu) has developed whole-body patient or worker anatomical models for Monet Carlo dose calculations. For this study, the model called VIP-Man that was developed from the segmented Visible Human images is used.

This paper presents the results of Monte Carlo secondary dose calculations to patients undergoing cancer treatment using the proton beams at the NPTC. Our emphasis is to evaluate the neutron dose and the implication for secondary cancer following proton therapy.

2. METHODS AND MATERIALS

2.1 The GEANT4 Code and Its Modifications

Developed with advanced software-engineering technologies, GEANT4 has many advantages over other general-purpose Monte Carlo codes [8]. Instead of being a standalone

executable, GEANT4 is a developing toolkit of C++ class libraries, covering various needs for solving particle transport problems. In using GEANT4, the user has to provide code to specify detector geometry, physics processes, source particle definition, and specific user actions. Compared to other Monte Carlo codes, the user of GEANT4 must have comprehensive knowledge about programming, particle physics, and Monte Carlo radiation transport theory. An advanced user often finds the flexibility offered by GEANT4 to be very attractive.

To improve the computational efficiency for patient-CT based simulations, we modified portions of the GEANT4 code for our applications. By implementing new algorithms to achieve faster particle transport in voxels and quicker geometry optimization, the proton Monte Carlo simulations with GEANT4 have been speeded up by 30 to 50 times. The modifications were carried out without compromising the accuracy in physics for protons and their secondaries. More details about Monte Carlo dose calculation in the GEANT environment are given elsewhere [6]. In our studies, a fairly good agreement between the Monte Carlo method and the pencil beam algorithm implemented in the CMS FOCUS program has been established, except in regions whose density is ~ zero (air). For the air regions, involved in cases such as paranasal sinus, the Monte Carlo method gives a lower dose estimate than the pencil beam algorithm.

2.2 The VIP-Man Model

The VIP-Man model is a segmented and labeled whole-body adult male patient anatomical model developed from the high-resolution transverse color photographic images of the Visible Human Project sponsored by the National Library of Medicine [9,10]. The availability of the Visible Human data set in the public domain makes it possible to use such images as a de facto standard human model for inter-comparison of treatment planning [11]. The segmented VIP-Man anatomical models contain the following organs or tissues: adrenals, bladder, esophagus, gall bladder, stomach mucosa, heart muscle, kidneys, large intestine, liver, lungs, pancreas, prostate, skeletal components, skin, small intestine, spleen, stomach, testes, thymus, thyroid, gray matter, white matter, teeth, skull CSF, stomach mucosa, male breast, eye lenses, and red bone marrow. The average tissue compositions and densities were used to tag each voxel in VIP-Man [12]. In previous studies, VIP-Man has been implemented into three Monte Carlo codes, EGS4, MCNP and MCNPX, to calculate organ doses for internal electrons [13], external photons [14], external electrons [15], external neutrons [16,17] and external protons. Since the organs have been segmented, organ doses can be determined precisely.

To implement the VIP-Man model into GEANT4, the voxel size was reduced from the original size of 0.33 mm × 0.33 mm × 0.33mm to 4 mm × 4 mm × 4 mm to facilitate Monte Carlo calculations [9]. The entire model thus includes 470 slices, each containing 86 × 147 or 12642 voxels, and the total number of voxels in the VIP-Man model is 6 millions. The anatomical data of the VIP-Man were stored in the same format as the patient CT data that are routinely used in our Monte Carlo treatment plan calculations. The same method developed at MGH was used to set up the position of the VIP-Man model based on field parameters, including gantry angle, couch angle, iso-center, and air gap.

One major difference between the VIP-Man model and a patient CT slice set is the way the electron density and tissue composition are defined. VIP-Man has been completely segmented, and is classified to 64 tissues/materials in GEANT4. The composition of VIP-Man tissues/materials is given by the ICRU [18]. In comparison, the information stored for each CT voxel is a Hounsfield number, which reflects the attenuation coefficient of tissues to diagnostic x-rays. A Hounsfield number to material conversion method has to be implemented (We adopted

the scheme by Schneider [19]). In principle, one material having a unique density has to be defined for each Hounsfield number, and hence a total of about 3000 materials will be defined.

2.3 Calculation of Organ Doses and Effective Dose

During simulations, the physical or absorbed dose in each voxel is accumulated. However, to evaluate the risk of radiation, the proton quality factors have to be applied to the physical dose to obtain the equivalent dose. Due to the dependence of the quality factors on dose, quality factors cannot be applied to absorbed dose on the fly. Neither could we record the energy distribution of protons and neutrons for each of the 6 million voxels in the VIP-Man model for post-processing, due to the unacceptable consumption of computer memory. In the current study, we adopted an approximate method. Instead of recording the particle energy distributions for each voxel, we only collected this information for each organ. We recorded the energy distribution of the neutrons crossing the organ surface (this is possible because the organs in VIP-Man are segmented). After simulations were done, an average neutron quality factor was calculated from the neutron energy distribution for each organ. The following ICRP-60 [20] neutron quality factors were employed in determining the average quality factors: Q = 5 for E_n < 10 keV; Q = 10 for 10 keV < E_n < 10 keV; Q = 20 for 100 keV < E_n < 2 MeV; Q = 10 for 2 MeV < E_n < 20 MeV; and Q = 5 for E_n > 20 MeV. This method should not be used for estimating the average quality factor of the primary proton beams. However, this study deals with organs located outside the irradiated target volume, and this method provides a reasonable approximation. Except for regions with very low density, the ranges of secondary and heavy charged particles in tissue (secondary protons, alphas, and recoil nuclei) are short, and doses to these organs comes primarily from the secondary neutrons.

In its 1990 recommendation, ICRP introduced the effective dose (E) as the primary dose limiting quantity and defined it as the sum of the weighted equivalent doses in twelve critical tissues and organs of the body and a “remainder” composed of additional organs [19]. The formalism is given by the expression:

$$E = \sum_T w_T H_T \qquad (1)$$

where w_T is the tissues weighting factor for tissue or organ T, and H_T is the equivalent dose in T defined as

$$H_T = \sum_R w_R D_{T,R} \qquad (2)$$

In this equation, $D_{T,R}$ represents the absorbed dose averaged over the organ T due to the radiation type R, and w_R is the radiation weighting factor (we used the quality factors as the radiation weighting factors in this study instead). The ICRP 60 organ weighting factors (0.2 to gonads, 0.12 to red bone marrow, colon, lung, and stomach, 0.05 to bladder, breast, liver, esophagus, and thyroid, 0.01 to bone surface and skin, and 0.05 to reminder organs) were adopted to convert equivalent dose to effective dose. The “reminder” contains the following organs in the calculation of the whole body effective dose: adrenals, brain, kidney, muscle, pancreas, small intestine, spleen, and thymus.

2.4 Case studies

Two proton therapy cases have been studied. The first one was a lung tumor case, featuring low-density soft tissue; the second was a paranasal sinus (PNS), presenting large air cavities. These impose challenges to treatment planning programs based on deterministic dose calculation methods.

The plan for the lung tumor consisted of three fields: LP (left posterior), RP (right posterior), and LA (left anterior). A more complicated five-field plan was designed for the PNS patient. However, only the three major fields were studied: AP (anterior posterior), LL (left lateral), and RL (right lateral); the other two patch fields were omitted. The voxel dimensions are 0.977 mm × 0.977 mm × 2.5 mm for the lung tumor patient, and 2 mm × 2 mm × 2.5 mm for the PNS patient. The planned GTV dose for the lung tumor is 72 Gy, and 45 Gy for the PNS patient. For each plan, a point in VIP-Man at a similar position as the tumor in the patient was selected. For example, for the lung tumor case, the iso-center was located inside the left lung and close to the chest wall of VIP-Man. With such a method, the distance from the iso-center to the outmost skin of VIP-Man may be different from that planned for patients. Therefore, different dose delivered to the target in VIP-Man when compared to the prescribed dose can be expected.

All simulation jobs were submitted to a Linux cluster at MGH. Each CPU in the cluster is equipped with 2G bytes of memory to satisfy the storage requirement for loading in anatomical information and dynamic memory assignment in C++ programs. The simulation for each field was performed in two steps. In the first step, the entire proton treatment nozzle was modeled [21], and the patient specific settings of the treatment nozzle were simulated. A phase space file recording protons and secondary neutrons reaching the nozzle exit is created. This phase space file was used as the particle source in the second step, in which VIP-Man was modeled and appropriately positioned. The second step conducted dose simulation in VIP-Man, and the output was a binary file in which the absorbed dose in each of the six million voxel. Totally, 100 million and 140 million protons from the phase space files were transported for the lung tumor plan and the PNS plan, respectively. In all simulations, protons (primary and secondary) and secondary neutrons were transported in full details, the energy of other secondaries (heavy recoil nuclei, electrons, and photons) are simply deposited locally. The collected information included the absorbed dose in each VIP-Man voxel and the neutron flux at the surface of each organ for converting absorbed dose to equivalent dose.

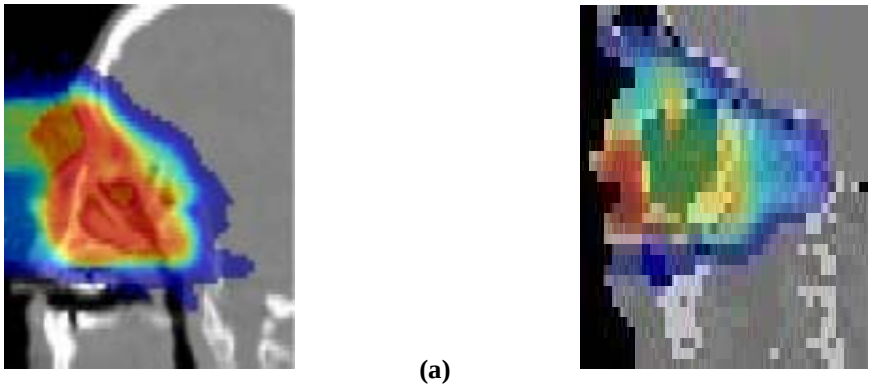

(a) **(b)**

Figure 1. Monte Carlo simulated dose distributions in (a) patient and (b) VIP-Man for the PNS plan

3. RESULTS AND DISCUSSIONS

Figure 1 illustrates the dose distributions in the patient and VIP-Man, after the application of the same PNS proton treatment plan to the patient and VIP-Man. Compared to figure 1(a), the composite dose distribution in figure 1 (b) is significantly distorted due to the large difference in anatomical structures between VIP-Man and the patient, which suggests again that this investigation is only applicable for low radiation doses induced by secondary particles outside of

the path of primary proton beams. Compared to dose deposition in the treatment region, the secondary doses in organs far from the tumor are much less dependent on the anatomy due to the large mean free path of secondary neutrons.

Figures 2 and 3 present the energy distribution of secondary neutrons arriving at several organs. The numbers of secondary neutron have been normalized by the number of protons entering into VIP-Man. The normalized total number of neutrons entering the major organs, together with the corresponding average quality factor estimated from neutron fluence and the average absorbed organ dose due to secondary particles, are summarized in Table I. For all organs, despite of a wide energy spread (up to 100 MeV), a large fraction of the neutrons (60% - 80%) are at energy less than 10 keV (corresponding to the large peak appearing in the leftmost energy bin in Figures 2 and 3). The existence of a large number of low/thermal energy neutrons is indicative of neutron elastic scattering in the patient body.

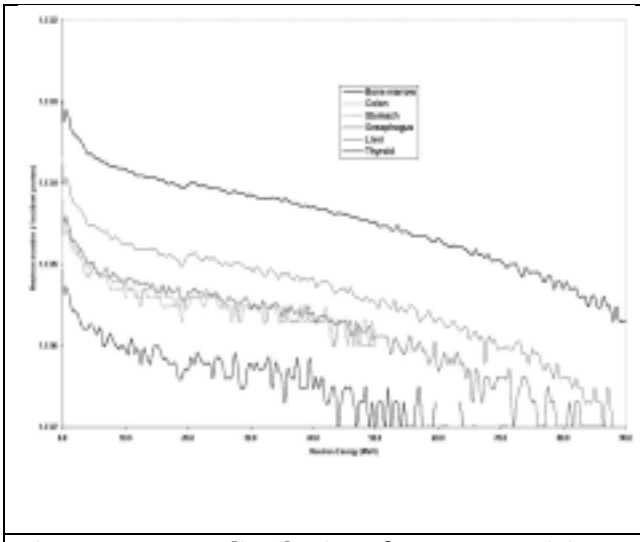

Figure 2. Energy distribution of neutrons arriving at the outer surface of some major organs under the lung tumor plan.

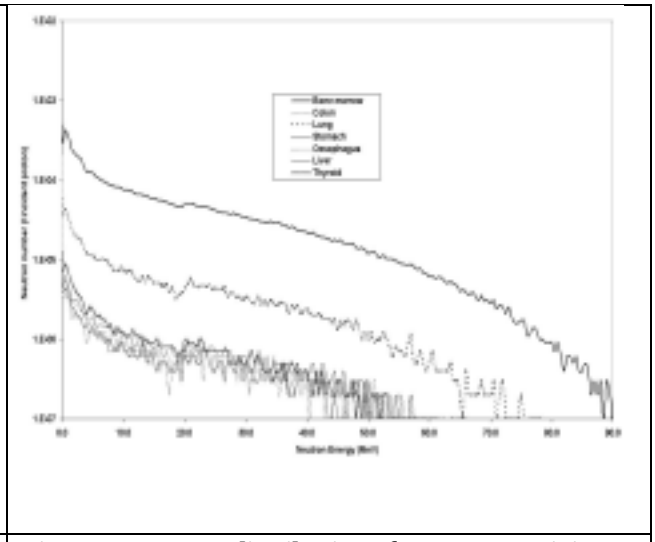

Figure 3. Energy distribution of neutrons arriving at the outer surface of some major organs under the PNS plan.

According to the theory of neutron elastic scattering, the average kinetic energy lost by a neutron in an elastic scattering with a static nucleus is a fixed fraction of the incident neutron energy. Consequently, in a relatively small number of scatterings, a high-energy neutron loses most of its kinetic energy. Afterwards, it becomes more and more difficult for the neutron to lose energy. Soft tissues are good neutron moderators, causing a significant number of low energy neutron to scatter before being captured. These low energy neutrons dominate the estimated quality factor. From Table I, the quality factors mainly distributed between 6 to 7 (the quality factor for neutrons of less than 10 keV energy is 5). As to the total number of neutrons, the organs/tissues can receive between 10-7 to 10-2 to neutrons per primary proton entering into VIP-Man, depending on the location (relative to the therapy volume) and the surface area of an organ. As a result of the relative large distance from the irradiated volumes, in both cases organs like bladder, testes, rectum and prostate are basically exempt from secondary particles. In contrast, organs/tissues within or closer to the tumor sites like liver, lung, heart, and parts of red bone marrow, are much more likely affected by the secondary irradiation.

Table I. Number of neutrons, quality factor and absorbed dose for different organs

Organ	Lung tumor plan			PNS plan		
	# of neutrons (per proton)	Quality factor	Absorbed dose (Gy)	# of neutrons (per proton)	Quality factor	Absorbed dose (Gy)
Adrenal	2.38e-4	5.8	4.46e-4	1.93e-5	5.7	3.50e-6
Bladder	2.96e-5	5.5	2.90e-5	3.00e-6	5.8	6.99e-7
Bone	6.11e-2	7.1	1.39e-2	5.69e-2	8.3	6.80e-3
Brain	1.02e-3	6.9	1.56e-4	3.86e-2	7.6	1.60e-3
Breast (male)	1.77e-4	7.3	1.30e-3	2.86e-5	8.2	8.64e-5
Colon	2.83e-3	5.8	4.46e-5	3.07e-4	6.0	2.13e-6
Esophagus	1.98e-3	6.5	2.20e-3	3.32e-4	6.3	6.93e-5
Eye lens	1.40e-6	6.3	7.01e-5	1.91e-4	9.5	1.35e-1
Heart	7.26e-3	6.4	1.63e-3	8.58e-4	6.3	3.30e-5
Kidneys	1.39e-3	5.7	2.68e-4	1.23e-4	5.7	5.60e-6
Liver	6.72e-3	6.3	1.40e-3	4.53e-4	6.1	1.39e-5
Lungs	2.39e-2	6.8	3.53e-2	2.38e-3	6.4	4.71e-5
Muscle	1.54e-1	7.2	2.15e-2	7.73e-2	8.1	2.00e-3
Pancreas	6.56e-4	5.8	4.19e-4	6.36e-5	5.8	9.50e-6
Prostate	6.20e-6	5.4	1.01e-5	8.00e-7	5.4	4.75e-7
Red bone marrow	3.11e-2	7.0	2.53e-2	1.23e-2	7.8	2.90e-3
Skin	9.11e-3	8.2	8.60e-3	9.70e-3	9.2	2.70e-3
Small intestine	2.42e-3	5.7	1.50e-4	2.78e-4	5.9	5.48e-6
Spleen	9.16e-4	5.9	4.07e-4	1.16e-4	6.0	1.30e-5
Stomach	2.95e-3	5.9	5.06e-4	3.66e-4	6.0	1.57e-5
Testes	1.10e-6	6.2	1.95e-6	1.00e-7	7.6	2.79e-8
Thymus	3.87e-4	6.4	2.00e-3	6.03e-5	6.6	6.71e-5
Thyroid	2.96e-4	6.4	1.30e-3	3.19e-4	7.1	3.80e-4

Illustrated in Table II are the voxel dose distributions in major organs/tissues for both plans, providing an explicit indication of the dose uniformity in each organ. As shown, except for the eye lens under the PNS plan, the neutron-induced average secondary doses in major healthy organs/tissues are at least three orders of magnitude lower than the planned GTV (gross tumor volume) dose. The dose to the eye lens under the PNS plan is distinctly higher (10^{-1} Gy), and the explanation is that the entire volume of the eye lens is close to the irradiated volume of the primary proton beams. The voxels in the healthy organs can receive very non-uniform dose depositions. The majority of the voxels of organs listed in Table II receive 0 or very low dose (1 mGy). However, a small volume fraction of the red bone marrow and lungs received over 0.1 Gy in the lung tumor case. The only exception is again the eye lens, for which over 50% of the voxels receive a dose larger than 0.1 Gy.

Table III presents the equivalent dose (for an organ) and effective dose (for the whole body) calculated using the estimated neutron quality factors in Table I and the ICRP-60 organ weighting factors. From Table III, the total effective dose due to secondary neutrons is low for both plans. The reading of the total effective dose is 0.058 Sv (5.8 rem) and 0.004 Sv (0.4 rem), respectively. That the effective dose for the lung tumor plan is one order of magnitude higher

than that for the PNS plan is apparently because of the closeness of major organs with a large tissue weighting factor to the irradiated lung tumor volume. The highest organ equivalent doses from the lung tumor plan are for the red bone marrow (0.177 Sv or 17 rem) and lungs (0.24 Sv or 24 rem). About 1% of the marrow volume received nearly 10 Sv equivalent dose from neutrons, which could cause secondary leukemia. For the PNS plan, several organs received relatively high equivalent doses. Although a patient is not subjected to radiation protection dose limits, it is worth to point out that the annual occupational limits recommended by the ICRP is 0.02 Sv (2 rem) for the effective dose and 0.5 Sv for the organ equivalent dose [20].

Table II. Fraction of organ voxels receiving doses in four dose intervals (%)

Organ	Lung tumor plan				PNS plan			
	0 – 0.001 Gy	**0.001-0.01 Gy**	**0.01 – 0.1 Gy**	**> 0.1Gy**	**0 – 0.001 Gy**	**0.001-0.01 Gy**	**0.01 – 0.1 Gy**	**> 0.1Gy**
Adrenal	86.2	13.8	0	0	100.0	0	0	0
Bladder	98.6	1.5	0	0	100.0	0	0	0
Bone	88.2	7.2	2.1	2.5	95.3	2.6	0.9	1.2
Brain	94.4	5.6	0	0	62.4	35.6	1.9	0.1
Breast (male)	64.1	35.4	0.5	0	1	0	0	0
Colon	94.5	1.5	0	0	100.0	0	0	0
Esophagus	38.0	61.7	0.3	0	100.0	0	0	0
Eye lens	93.7	6.3	0	0	0	12.5	31.3	56.3
Heart	54.3	44.9	0.8	0	100.0	0	0	0
Kidneys	91.0	9.0	0	0	100.0	0	0	0
Liver	59.4	40.2	0.4	0	100.0	0	0	0
Lungs	36.6	36.7	17.2	9.5	99.9	0.1	0	0
Muscle	82.7	10.5	3.2	3.7	98.5	0.9	0.2	0.4
Pancreas	86.0	14.0	0	0	100.0	0	0	0
Prostate	99.7	0.3	0	0	100.0	0	0	0
Red bone marrow	76.4	15.7	3.9	4.1	97.4	1.7	0.3	0.5
Skin	85.9	10.3	1.7	2.2	95.7	3.1	0.5	0.7
Small intestine	94.8	5.2	0	0	100.0	0	0	0
Spleen	85.9	14.1	0	0	100.0	0	0	0
Stomach	82.3	17.8	0	0	100.0	0	0	0
Testes	100.0	0	0	0	100.0	0	0	0
Thymus	36.0	63.0	1.0	0	100.0	0	0	0
Thyroid	58.7	41.3	0	0	95.6	4.4	0	0

Table III. Calculated equivalent doses and effective dose for two proton treatment plans (Equations 1 & 2 were used in the calculations)

			ICRP60 organ/tissue weighting factors*	Lung tumor plan	PNS plan
Equivalent dose (Sv)	Testes (Gonads)		0.2	1.21e-5	2.12e-7
	Red bone marrow		0.12	1.77e-1	2.26e-2
	Colon		0.12	2.59e-4	1.28e-5
	Lung		0.12	2.40e-1	3.01e-4
	Stomach		0.12	2.99e-3	9.42e-5
	Bladder		0.05	1.60e-4	4.05e-6
	Breast		0.05	9.49e-3	7.08e-4
	Liver		0.05	8.82e-3	8.48e-5
	Esophagus		0.05	1.43e-2	4.37e-4
	Thyroid		0.05	8.32e-3	2.70e-3
	Bone surface		0.01	9.87e-2	5.64e-2
	Skin		0.01	7.05e-2	2.48e-2
	Reminder organs	Muscle	0.025	1.55e-1	1.62e-2
		Brain	0.025	1.08e-3	1.22e-2
		Kidneys		1.53e-3	3.19e-5
		Adrenals		2.59e-3	2.00e-5
		Pancreas		2.43e-3	5.51e-5
		Small intestine		8.55e-4	3.23e-5
		Spleen		2.40e-3	7.80e-5
		Thymus		1.28e-2	4.43e-4
Effective dose (Sv)				5.81e-02	4.22e-03

*The effective dose calculation follows a revised ICRP 60 recommendation

The results suffer from the statistic errors or uncertainties. As already mentioned, 10^8 and 1.4×10^8 protons were transported for the lung tumor plan and the PNS plan, respectively. Therefore, the dose estimate for organs/tissues that receive 10^{-2} to 10^{-3} neutron/proton (e.g. the red bone marrow and the brain) is quite reliable. On the other hand, the results for small organs such as prostate and testes that received only 10^{-6} to 10^{-7} neutrons/proton have a large statistic error. Effective dose is derived primarily from organs/tissues like lungs and red bone marrow for which dose is accurately calculated. The statistical uncertainties for this calculated total effective dose is only 0.5% for both plans.

4. CONCLUSIONS

The Monte Carlo method is an effective tool for secondary dose calculation in patient geometry. We presented results of effective doses calculated using the GEANT4 code for two proton treatment plans on the VIP-Man whole body model. Due to the significant differences in anatomic structures between VIP-Man and the patients for which the treatment plans were made, the primary dose distributions in VIP-Man differ significantly from the planned dose distributions in patients. Therefore, the approach of adopting VIP-Man as the image-based model is only meaningful for studying dose to organs located outside the planned target volume.

The magnitude of secondary dose in organs/tissues depends on the distance of the organs/tissues to the irradiated volume of the primary proton beams. Generally, the averaged secondary dose is three or more orders of magnitudes lower than the planned dose in GTV. The neutron quality factor is around six since the neutron fluence includes a large fraction of thermal and low energy neutrons. For the two lung tumor and PNS proton treatment plans considered in this study, the overall whole body effective dose is 0.058 Sv (5.8 rem) and 0.004 Sv (0.4 rem), respectively.

5. ACKNOWLEDGMENTS

Dr. Harald Paganetti was supported in part by grant CA 21239 from the National Cancer Institute, National Institute of Health.

6. REFERENCES

1.“Introduction to Cancer Therapy (Radiation Oncology),” http://www.radiologyinfo.org/content/therapy/about_oncology.htm (2004).
2. http://press2.nci.nih.gov/sciencebehind/cancer/cancer25.htm .
3. P. Okunieff, D. Morgan, A. Niemierko and H. Suit, “Radiation dose response of human tumors,” *Int. J. Radiat. Oncol., Biol., Phys.* **32**, pp. 1227-1237 (1995).
4. U. Schneider, S. Agosteo, E. Pedroni, J. Besserer, “Secondary neutron dose during proton therapy using spot scanning,” *Int. J. Radiat. Oncol., Biol., Phys.* **53**, pp. 244-251 (2002).
5. X. Yan, U. Titt, A. M. Koehler and W. D. Newhauser, “Measurement of neutron dose equivalent to proton therapy patients outside of the proton radiation field,” N*ucl. Inst. and Meth. in Phys. Res.* **A476** pp. 429-434 (2002)
6. H. Jiang and H. Paganetti, “ Adaption of GEANT4 to Monte Calro dose calculations based on CT data,” *Med. Phys.*, **31** pp. 2811-2818 (2004).
7. H. Paganetti, H. Jiang, E. Rietzel, J. Adams and G. T. Chen, “The potential of four-dimensional Monte Carlo dose calculation for investigating organ motion effects with high temporal resolution,” *Int. J. Radiat. Oncol., Biol., Phys.* **60**, pp. 942-950 (2004).
8. S. Agostinelli et al., “GEANT4—A simulation toolkit,” *Nucl. Instrum. Methods Phys. Res. A* pp. 506, 250–303 (2003).
9. X. G. Xu, T. C. Chao and A. Bozkurt , “VIP-MAN: an image-based whole-body adult male model constructed from color photographs of the Visible Human Project for multi-particle Monte Carlo calculations,” *Health Phys.* **78** pp.476-85 (2000).
10. V. M. Spitzer and D. G. Whitlock, *Atlas of the Visible Human Male,* Jones and Bartlett Publishers (1998).
11. J. S. Aldridge, P. J. Reckwerdt and T. R. Mackie, “A proposal for a standard electronic anthropomorphic phantom for radiotherapy,” *Med. Phys.* **26**, pp. 1901-3 (1999).
12. International Commission on Radiological Protection, *Report of the Task Group on Reference Man*, Pergamon Press, Oxford UK (1975).
13. T. C. Chao and X. G. Xu, “Specific absorbed fractions from the image-based VIP-Man body model and EGS4-VLSI Monte Carlo code: Internal electron emitters,” *Phys. Med. Biol.* **46** pp.901-27 (2001).

14. T. C. Chao, A. Bozkurt and X. G. Xu, "a Conversion coefficients based on the VIP-Man anatomical model and GS4-VLSI code for external monoenergetic photons from 10 keV to 10 MeV," *Health Phys.* **81** pp.163-83 (2001).
15. T.C. Chao, A. Bozkurt and X. G. Xu, "Organ dose conversion coefficients for 0.1- 10 MeV external electrons calculated for the VIP-Man anatomical model," *Health Phys.* **81** pp.203-14 (2001).
16. A. Bozkurt, T. C. Chao and X. G. Xu, "Fluence-to-dose conversion coefficients from monoenergetic neutrons below 20 MeV based on the VIP-Man anatomical model," *Phys. Med. Biol.* **45** pp. 3059-79 (2000).
17. A. Bozkurt A, T. C. Chao and X. G. Xu, "Fluence-to-dose conversion coefficients based on the VIP-Man anatomical model and MCNPX code for monoenergetic neutrons above 20 MeV," *Health Phys.* **81** pp. 183-202 (2001).
18. International Commission on Radiation Units and Measurements, *Tissue substitutes in radiation dosimetry and measurement*, ICRU Publications, Bethesda MD (1989).
19. W. Schneider, T. Bortfeld and W. Schlegel, "Correlation between CT numbers and tissue parameters needed for Monte Carlo simulations of clinical dose distributions," *Phys. Med. Biol.* **45** pp. 459-478 (2000).
20. International Commission on Radiological Protection, *1990 recommendations of the International Commission on Radiological Protection*, Pergamon Press, Oxford UK (1991).
21. H. Paganetti, H. Jiang, S.-Y. Lee and H. Kooy, "Accurate Monte Carlo simulations for nozzle design, commissioning, and quality assurance in proton radiation therapy," *Med. Phys.*, **31** pp. 2107-2118 (2004)